

Sol-gel processing of lithium disilicate

Part II *Crystallization and microstructure development of coatings*

P. LI, L. F. FRANCIS

Department of Chemical Engineering and Materials Science, University of Minnesota, Minneapolis, MN 55455, USA

Lithium disilicate ($\text{Li}_2\text{Si}_2\text{O}_5$) coatings were prepared by spin-coating alkoxide solutions on to substrates [Si, SiO_2 , polycrystalline (poly) Si, sapphire] and heating isothermally at 500–600 °C. The effects of solution chemistry, coating thickness and substrate type on crystallization behaviour and microstructure development were investigated using atomic force microscopy, X-ray diffraction and transmission electron microscopy. Amorphous dried coatings began to crystallize into $\text{Li}_2\text{Si}_2\text{O}_5$ at 500–550 °C. Coatings prepared on Si substrates (with a thin native oxide) using Li–Si methoxyethoxide solution crystallized into microstructures with large grain sizes (ca. 2–5 μm diameter) as compared with the coating thickness ($< 0.3 \mu\text{m}$). Nucleation rate in these coatings could be increased (and hence transformation rate increased and grain size decreased) by: (1) adding H_2PtCl_6 to the solution to act as nucleation agent; (2) increasing the thickness of the coating; or (3) using a crystalline substrate (sapphire or poly Si). Coatings prepared using Li–Si ethoxide solution had fine-grained microstructures ($\leq 0.5 \mu\text{m}$ diameter) for all substrates. Chemical heterogeneity in the ethoxide system may have increased nucleation rate. Nucleation rate in this system could be decreased by using partially hydrolysed tetraethylorthosilicate as the Si precursor. The relationship between solution chemistry and microstructure was used to tailor microstructures in multilayer coatings.

1. Introduction

Many microstructural characteristics of sol-gel-derived coatings, including crystalline phase content, grain size and porosity, develop during crystallization. These microstructural features impact the properties and performance of the coating. For example, ultra-fine-grained barium titanate thin films do not display ferroelectricity [1], the presence of a second phase in the lead-magnesium niobate titanate thin layers lowers the dielectric constant [2] and porosity degrades the corrosion resistance of protective ceramic coatings on steel [3]. In the preparation of a coating by the sol-gel route several processing steps bring about chemical and microstructural changes [4, 5]. First, an amorphous coating is formed by depositing a metallorganic or colloidal sol on to a substrate. During the deposition, the liquid sol transforms into a solid layer by a combination of drying and reaction [6] or by aggregation. Then, a variety of processes take place during thermal treatment of the coating. Drying, pyrolysis, structural relaxation and viscous sintering all occur at fairly low temperatures (typically $< 400 \text{ }^\circ\text{C}$) while the coating is still amorphous. At higher temperatures the coating crystallizes; the crystalline microstructure can be further modified by sintering and grain growth. This report focuses specifi-

cally on the impact of crystallization behaviour on coating microstructure.

The development of crystalline microstructures in sol-gel-derived coatings is affected by processing parameters: precursor solution chemistry, substrate characteristics, deposition conditions and thermal processing conditions. For example, Joshi and Mecartney [7] found that the amount of water added to a lithium niobium alkoxide precursor solution influenced the coating porosity and grain size, and Keddie *et al.* [8] and Schwartz *et al.* [9] showed that using a faster heating rate delays crystallization in sol-gel-derived coatings. Optimizing the processing parameters and understanding the physical and chemical changes that accompany the various stages of the sol-gel process will improve control of the final microstructure and reproducibility. Since important microstructural features develop during the crystallization step, a better understanding of how to control crystallization and the resulting microstructure will benefit processing technologies used for many applications of sol-gel coatings.

In this study, lithium disilicate ($\text{Li}_2\text{Si}_2\text{O}_5$) coatings were prepared from alkoxide solutions. The effects of solution chemistry, substrate material, coating thickness and thermal treatment on crystallization

behaviour and microstructure development were investigated. Lithium disilicate was chosen for its scientific interest in crystallization studies [10,11] and technological importance as a glass-ceramic [12,13], pyroelectric glass-ceramic [14], dental material [15] and fast-ion conductor [16]. Additionally, the amorphous-to-crystalline phase transformation is relatively slow at intermediate temperatures (450–550 °C) so that partially crystallized microstructures can be studied. Thus, lithium disilicate coatings offer an opportunity to understand the relationships between sol-gel processing conditions, crystallization behaviour and the resulting microstructure. We are not aware of any reports concerning the processing and crystallization behaviour of sol-gel-derived lithium disilicate coatings; however, bulk sol-gel-derived lithium disilicate has been studied, as reviewed previously [17].

In part I of this series, we reported on the crystalline phase development in sol-gel-derived powders prepared using different alkoxide-based solution systems [17]. A system using lithium nitrate as one of the precursors was unsatisfactory because lithium nitrate recrystallized in the dried gel. Difficulties were also encountered with an ethoxide-based solution system; lithium hydroxide precipitated and then redissolved during the sol-to-gel transition. Gels prepared from the nitrate and ethoxide routes crystallized into a combination of lithium metasilicate (Li_2SiO_3) and the desired lithium disilicate. Three solution routes produced nearly single phase lithium disilicate: (1) Li-Si ethoxide solution with HNO_3 additive; (2) Li-Si ethoxide solutions prepared by combining partially hydrolysed TEOS with lithium alkoxide; and (3) Li-Si methoxyethoxide solution. In this report, we continue the investigation by studying the crystallization and microstructure development of coatings prepared using these solution routes.

2. Experimental procedure

2.1. Coating preparation

Li-Si alkoxide stock solutions were prepared by mixing equimolar amounts of lithium methoxide and TEOS in an alcohol (ethanol or 2-methoxyethanol), followed by refluxing and distillation, as detailed in part I [17]. Alkoxide stock solutions were combined with hydrolysis solutions (containing water and solvent) to form solutions suitable for coating. After preliminary investigations of solution viscosity, coating quality and consistency, the following solution conditions were chosen: concentration of $[\text{Li}] = [\text{Si}] = 0.375 \text{ M}$ and hydrolysis ratio (r) ($[\text{H}_2\text{O}]/[\text{Si}] = 2$). Coating solutions were aged for 1 h (methoxyethoxide) or overnight (ethoxide). A longer ageing time was used for the ethoxide system to allow dissolution of the LiOH precipitate and potentially enhance chemical homogeneity [17]. The effect of a nucleating agent was investigated by adding a small amount of H_2PtCl_6 to the hydrolysis solution used to prepare the Li-Si methoxyethoxide coating solution ($[\text{Pt}]/[\text{Si}] = 0.0055$). Also, an ethoxide solution was synthesized using partially hydrolysed TEOS ($r = 1$) as a Si precursor, as described previously [17].

Coatings were prepared on several substrate materials. Most experiments were carried out using single crystal Si substrates with (1 0 0) orientation. Substrates were cleaned thoroughly (see below), but the native oxide was not removed. Other substrates included (1 0 0) Si with a thermally-grown oxide layer (ca. 100 nm), (1 0 0) Si with a layer of polycrystalline Si (ca. 550 nm) deposited by low-pressure chemical vapour deposition and (0 0 0 1) sapphire. Some sapphire substrates were annealed for 2 h at 1400 °C. Coatings were prepared on $1 \times 1 \text{ cm}$ square substrate pieces or circular (1 inch diameter) sapphire pieces. Immediately before deposition, substrates were ultrasonically cleaned successively in trichloroethylene, acetone and isopropyl alcohol (each for 10 min), and blown dry with compressed air.

Coating solutions were syringed through $0.2 \mu\text{m}$ filters on to substrates, spin cast (2000 r.p.m., 1 min) and then dried on a hot plate (150 °C for ethoxide coatings, 200 °C for methoxyethoxide). To build up a thicker coating, several layers (up to six) were deposited with hot-plate drying between depositions. After drying, coatings were amorphous; several heating procedures were used to investigate crystallization. Isothermal heat treatments were carried out at 500, 525, 550, 575 and 600 °C for times typically ranging from 15 to 120 min. In an isothermal heating, the specimen was set in a preheated alumina boat and placed into a preheated box furnace. All heat treatments were carried out in air. Temperatures higher than 600 °C were not investigated due to greater lithium volatility [18] and possible reactions between the coating and substrates. After firing, specimens were stored in sealed containers. If exposed to air for several months the surface of the coating became cloudy, probably due to efflorescence from reaction with CO_2 [19].

2.2. Characterization

Microstructure evolution was mainly characterized by atomic force microscopy (AFM). AFM provides images of the surface topology and, for the lithium disilicate coatings described here, was better able to distinguish between the crystalline and amorphous regions of the coating than scanning electron microscopy (SEM). Another advantage of AFM was its ability to examine the same sample after successive heat treatments. (SEM requires a conductive coating which interferes with this type of analysis.) A Nanoscope III AFM was used in the constant force mode and with a scanning rate of 2 Hz (2 lines s^{-1}). In determining microstructure characteristics, such as the area fraction crystallized and the average grain size, several AFM images of the same sample were analysed.

Transmission electron microscopy (TEM; Philips CM30) was used to study planar microstructures, cross-sectional microstructures and the crystal structures of some coating-substrate combinations. Planar TEM samples were prepared by spin-coating the Li-Si alkoxide solutions ($[\text{Li}] = [\text{Si}] = 0.1 \text{ M}$, $r = 2$) on to a silica-coated gold TEM grid. The procedure for preparation of silica-coated TEM grids is

described by Wang *et al.* [20]. The silica layer was ca. 50 nm thick. Li–Si alkoxide solution was spin-coated on to the silica-coated grid and heat treated at 600 °C for 1 h. Cross-sectional TEM samples for coatings deposited on Si were prepared by gluing together two specimens with epoxy resin (M-bond 610 adhesive), separating the coatings face-to-face. The samples were held overnight with pressure applied to minimize the amount of epoxy resin between the two facing coatings [21]. The sample was polished (perpendicular to the interface) down to a thickness of 20–30 μm and then ion-beam thinned on both sides using a rotation stage (5 kV, 1.5 mA ion current per gun, incidence angle of 17°). Because lithium disilicate was removed at a slower rate than the silicon substrate, four sapphire blocks were set on both top and bottom of the TEM sample holder in a position parallel to the sandwiched films to prevent the preferential removal of the substrate.

Crystalline phase development was studied by X-ray diffraction (XRD; Rigaku D-Max). XRD was typically carried out over a 2θ range which included the most intense peaks for lithium disilicate and lithium metasilicate, but some investigations included scanning over wider angular ranges. Coating thickness was measured by ellipsometry and further checked by a cross-sectional field emission SEM (Hitachi S900) and cross-sectional TEM.

3. Results

3.1. Methoxyethoxide solution deposited on Si

The early stages of crystallization in coatings prepared using Li–Si methoxyethoxide solution are shown in Fig. 1. These coatings were fabricated using four depositions of coating solution and had a final thickness of ca. 0.2 μm . After low-temperature heating, the coating was amorphous and generally featureless except for a fine surface texture, (see Fig. 1a.) For the higher temperature heating conditions (Fig. 1b and c), the microstructures are partially crystallized with oval-shaped grains in a surrounding amorphous phase. The grains are few in number, but their lateral dimensions (0.2–1.0 μm) are greater than or equal to the coating thickness. As expected, coatings heated at 500 °C required a longer time to reach a similar state of crystallinity as those heated at 550 °C (8 h at 500 °C as compared with 25 min at 550 °C). From XRD and electron diffraction, the crystalline phase that forms is lithium disilicate (see below).

The morphology of the lithium disilicate crystalline phase was further studied using TEM of coatings deposited and heated on silica coated grids. Because a thin layer of native oxide is present on our Si substrates, the TEM observations are indicative of the behaviour we observed on Si. One deposition of a low concentration solution was used to prepare this

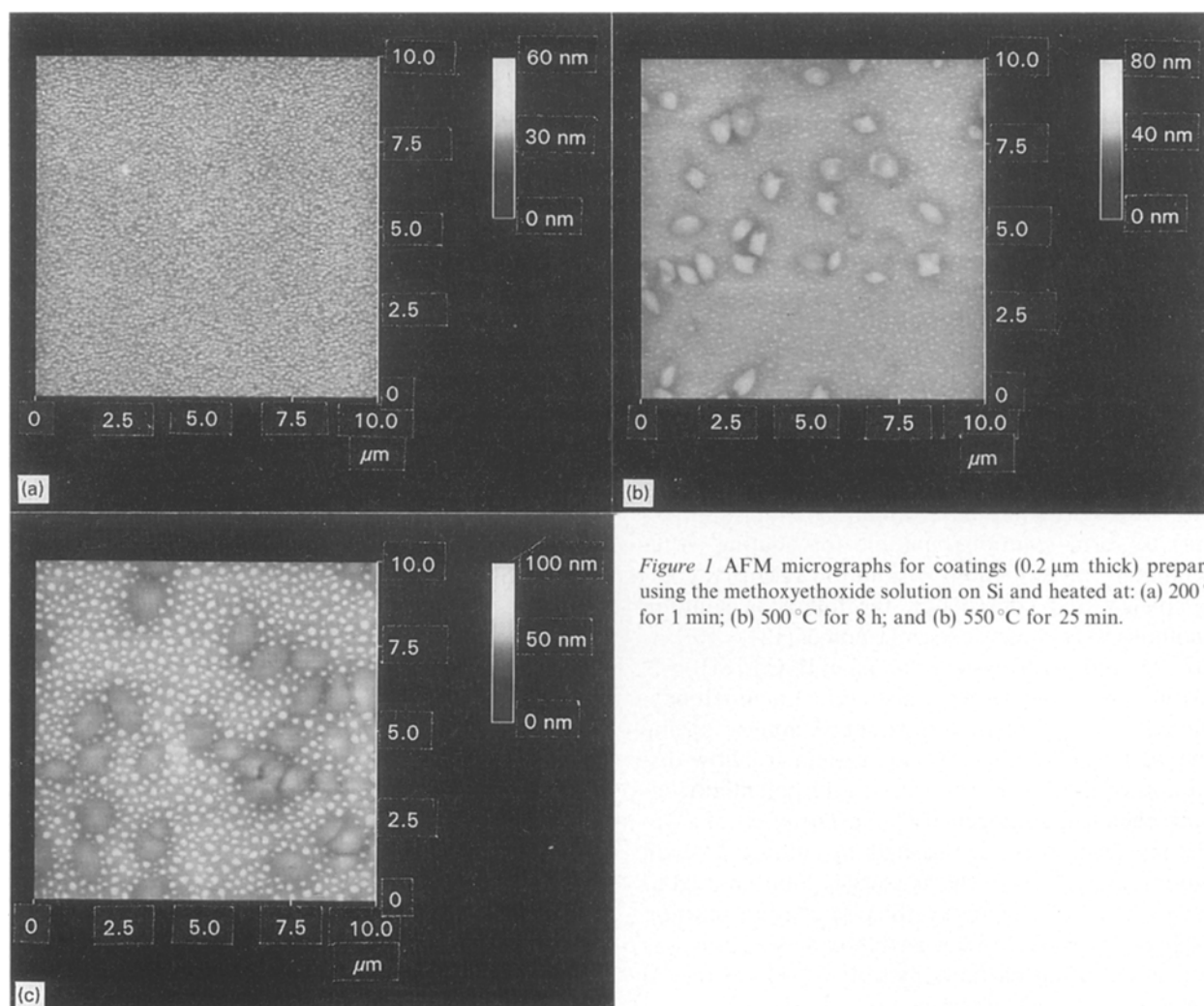


Figure 1 AFM micrographs for coatings (0.2 μm thick) prepared using the methoxyethoxide solution on Si and heated at: (a) 200 °C for 1 min; (b) 500 °C for 8 h; and (c) 550 °C for 25 min.

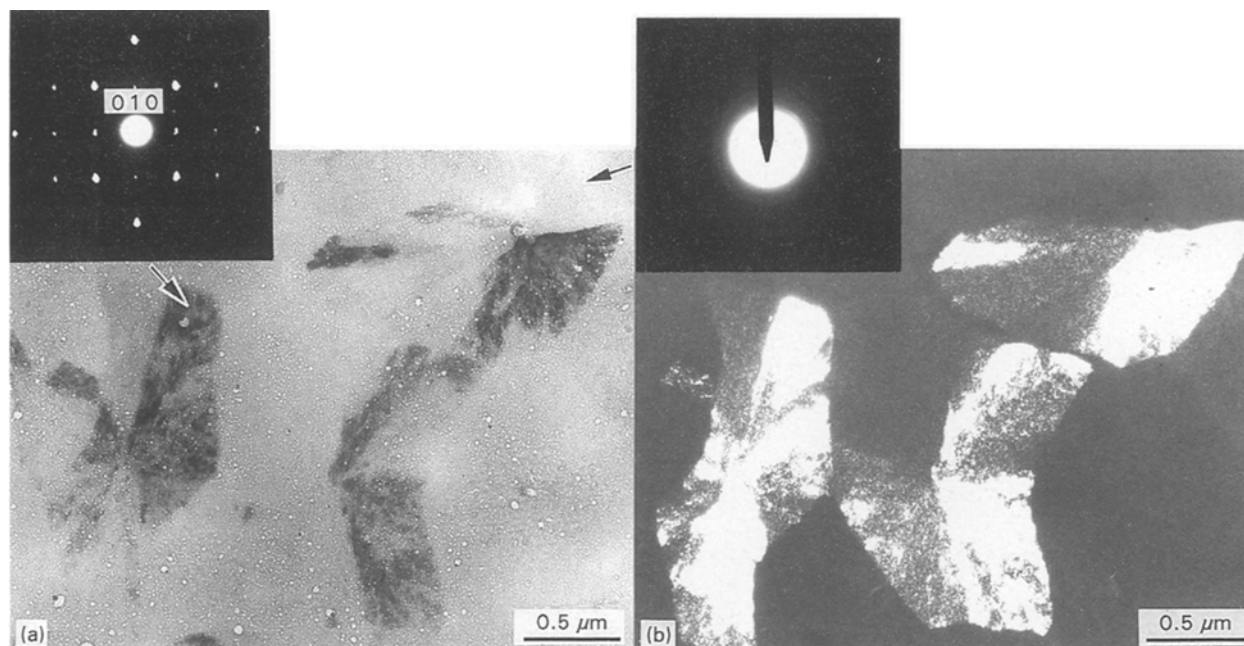


Figure 2 TEM micrographs of a coating prepared using methoxyethoxide solution ($r = 2$ and $[\text{Li}] = [\text{Si}] = 0.1 \text{ M}$) and heated at 600°C for 1 h. (a) Bright-field image with electron diffraction pattern from a crystalline region given in the inset and (b) dark-field image with electron diffraction pattern from a non-crystalline region given in the inset.

coating; therefore, the coating was very thin (ca. $0.02 \mu\text{m}$). Fig. 2 shows the coating microstructure which consisted of crystalline grains growing in an amorphous coating. An electron diffraction pattern from the crystalline region confirms that the crystalline phase is lithium disilicate with a zone axis of $[010]$ (inset Fig. 2a); amorphous material was also found by electron diffraction (inset Fig. 2b). The crystalline growth morphology follows a radiating, spherulitic pattern. This morphology is typical of bulk lithium disilicate [22,23], as well as other silicates [24]. The TEM dark-field image of the lithium disilicate crystals indicates that the orientation of the fibular extensions differs from one portion of the spherulite to the another. These coatings were damaged by exposure to the electron beam, making extensive TEM investigations difficult.

The effect of isothermal heating time at 550°C on the microstructure of a coating is illustrated in Fig. 3. The fraction of the surface area covered by lithium disilicate grains increases with isothermal hold time from ca. 0.30 after 30 min (not shown, but similar to Fig. 1c) to ca. 0.44 after 45 min (Fig. 3a), ca. 0.73 after 60 min (Fig. 3b) and fully crystallized after 90 min (Fig. 3c) at 550°C . The average size of the grains also increases with hold time. In these AFM experiments, the area fraction crystallized is determined by studying the surface of the coating. The area fraction is also a good indicator of the volume fraction crystallized for these samples. TEM cross-sectional analysis of a fully crystallized coating (Fig. 4) shows that the grains extend through the thickness of the coating with grain boundaries perpendicular to the coating surface. Therefore, the area fraction represents the lower bound on the volume fraction; the volume fraction would exceed the area fraction if the specimen had grains that had not yet emerged

through the surface. Further, our definition of full crystallization is impingement of spherulites; continued crystallization of the spherulite is possible if non-crystalline material remains between the radiating fibular extensions [25].

The isothermal heating temperature and coating thickness impact the crystallization kinetics and grain size. At 500°C crystallization is very slow and the coating is only slightly crystallized after 8 h (see Fig. 1a). Isothermal investigations, similar to those discussed above, were carried out on the coatings ($0.17 \mu\text{m}$ thick) at $525, 550, 575$ and 600°C ; the change in crystallinity and grain size are summarized in Fig. 5. At 525°C the amorphous-to-crystalline transformation is still slow, but crystalline grains appear after 90 min of heating. At 550°C the transformation is gradual and complete by 90 min. By contrast, at 575 and 600°C , the transformation is rapid; only 30 (at 575°C) and 15 min, respectively, were needed to reach full crystallization. The average grain size increased steadily during crystallization, but remained roughly constant after full crystallization and grain impingement (see Fig. 5b). Growth of crystalline grains in the amorphous phase is faster than grain growth after full crystallization. The effect of film thickness on the crystallization and microstructure development is summarized in Table I. Also, Fig. 6 shows AFM micrographs for identically treated coatings of different thicknesses. The number of grains per unit area, the area fraction crystallized and the size of the grains increase with the coating thickness. Overall, the data in Table I shows that thicker coatings transformed more rapidly and, in the end, developed into finer-grained microstructures rather than thinner coatings. The observation of a partially crystalline microstructure for the very thin coating used for TEM is consistent with this trend.

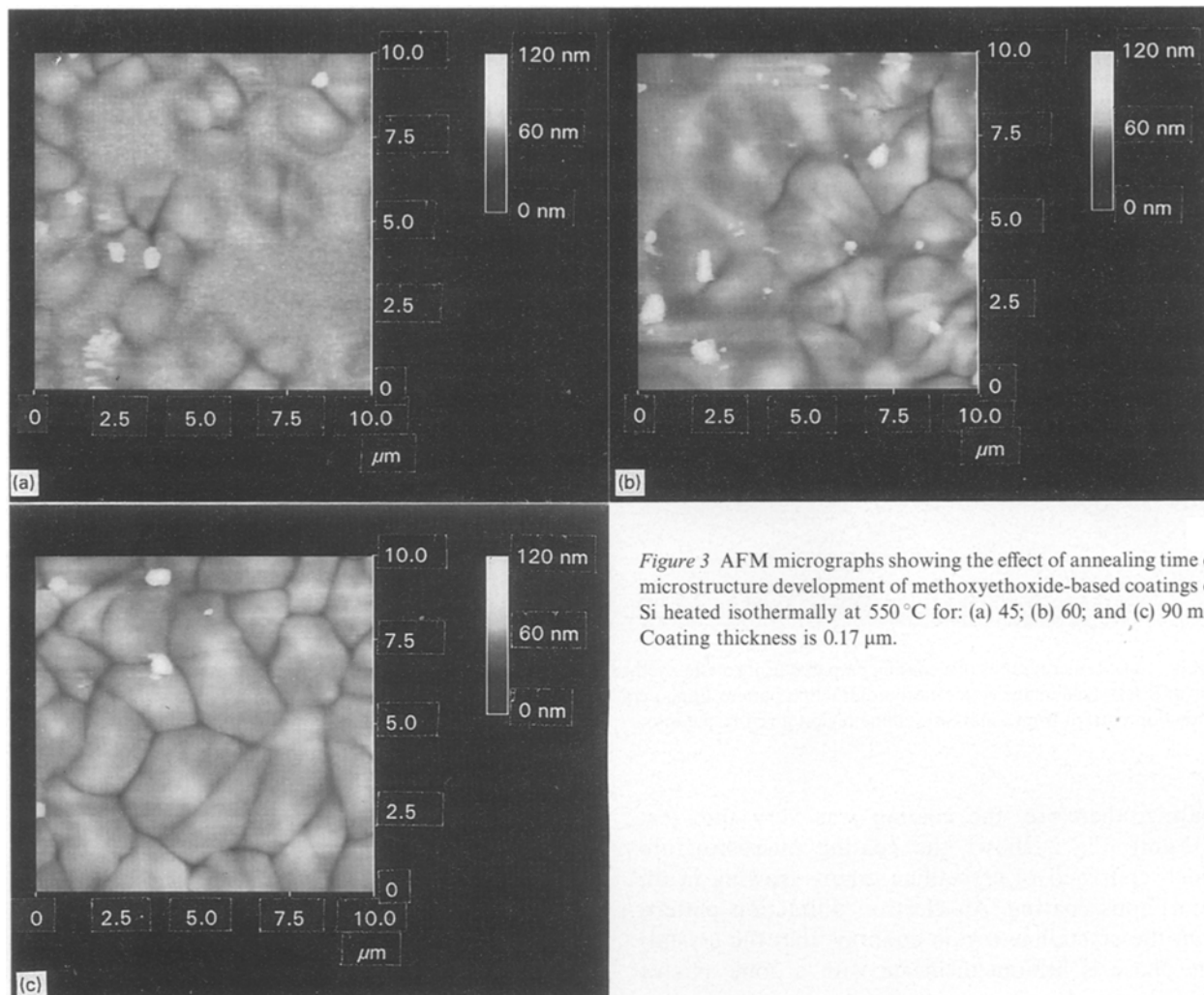


Figure 3 AFM micrographs showing the effect of annealing time on microstructure development of methoxyethoxide-based coatings on Si heated isothermally at 550 °C for: (a) 45; (b) 60; and (c) 90 min. Coating thickness is 0.17 μm .

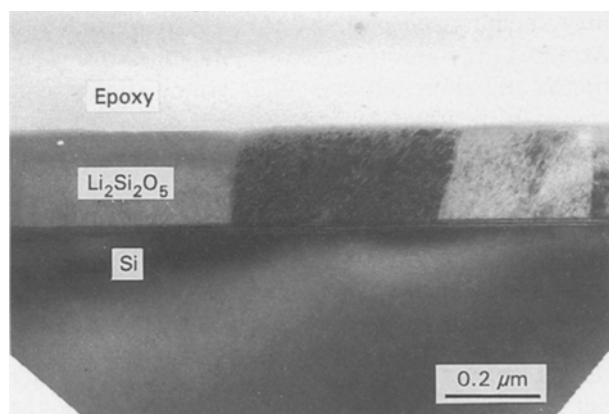


Figure 4 Cross-sectional TEM micrograph of a coating prepared using the methoxyethoxide solution and heated at 600 °C for 30 min.

Fig. 7 shows XRD results for the coatings heated at 550 °C. The fraction of crystalline phase increased with the annealing time. While the diffracted intensity from these thin samples is weak, the emergence of the lithium disilicate peaks is evident and peaks for lithium metasilicate (Li_2SiO_3) are absent (i.e. the strong peaks for Li_2SiO_3 occur at $2\theta = \text{ca. } 27$ and 33°). Gel-derived powders [17] prepared from the Li-Si

methoxyethoxide stock solution also form lithium disilicate without lithium metasilicate. The strongest lithium disilicate peak is (040) for coatings on Si substrates; other peaks [(130) and (111)] are not as intense as predicted from powder diffraction (JCPDS 17-447). The dominance of the (040) diffraction indicates a preference for the b -axis of the lithium disilicate structure to be perpendicular to the plane of the coating, which is consistent with TEM observations (i.e. zone axis of [010]). From the cross-sectional TEM micrograph, the contrast between adjacent grains shows that the in-plane orientation of a - and c -axes is random (see Fig. 4).

Coatings prepared on Si using the methoxyethoxide route inevitably developed into large-grained microstructures. A microstructure with a small grain size could be obtained by introducing a nucleating agent (H_2PtCl_6) into the coating solution before deposition. During thermal treatment, hydrogen and chlorine are removed, leaving behind small particles of platinum [26]. The platinum particles within the coating were too small to be identified by XRD or TEM techniques; however, their effect was evident. After heating the sample at 550 °C for 30 min, a fine-grained, fully crystallized microstructure was obtained (Fig. 8). Comparison with Fig. 3 shows that the increase in the nucleation rate with Pt addition allowed full crystallization to occur in a shorter time.

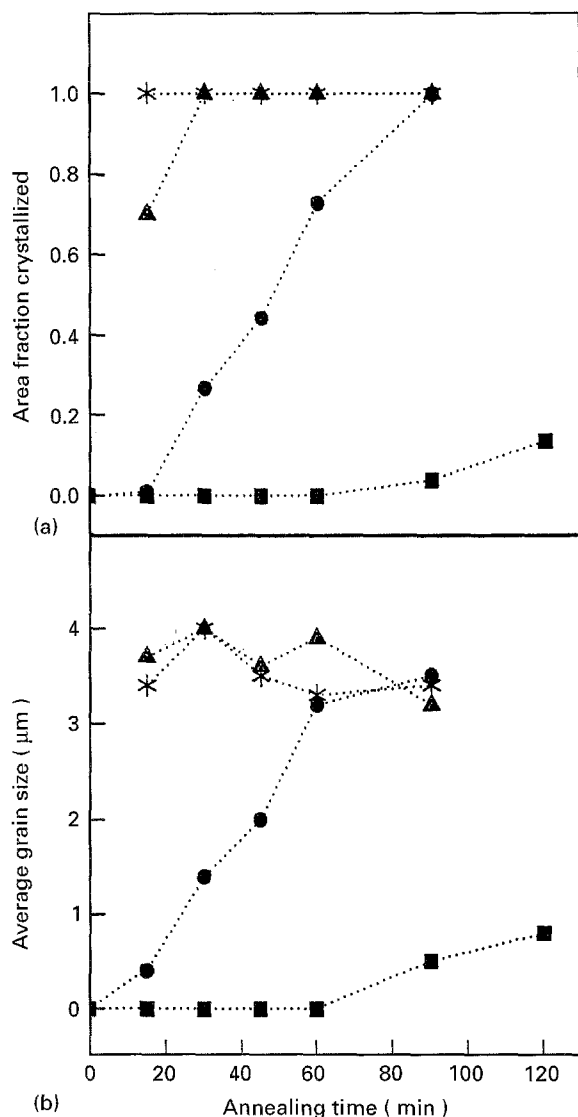


Figure 5 (a) Change in the area fraction of crystallized phase and (b) the average grain size with time for different isothermal heating temperatures. Coatings (0.17 μm thick) were prepared using the methoxyethoxide solution on Si. Data are average values measured from several AFM images. Temperature ($^{\circ}\text{C}$): ■, 525; ●, 550; ▲, 575; *, 600.

TABLE I Microstructure variations in methoxyethoxide coatings on Si heated at 550 $^{\circ}\text{C}$ for 30 min.

Coating thickness (μm)	Grain density (no. of grains/ m^2)	Area fraction crystallized	Average grain size ^a (μm)
0.04	0.66	0.04	1.0
0.08	0.97	0.11	1.5
0.14	2.50	0.36	1.9
0.28	2.81	0.39	1.9

^a Average grain size determined from measurement of the longest length of the grain.

3.2. Ethoxide solutions deposited on Si

AFM micrographs for coatings prepared on Si using the ethoxide route are given in Fig. 9. The coating solution was formulated without partial hydrolysis of TEOS or nitric acid addition. These coatings were prepared with four depositions of coating solution and had a thickness of ca. 0.15 μm . After a heat treatment at 500 $^{\circ}\text{C}$ for 1 h (Fig. 9a), the coating was amorphous

by XRD, but had developed coarse surface features. After a brief heating at 550 $^{\circ}\text{C}$ (15 min), a fine-grained ($<0.5 \mu\text{m}$), fully crystallized microstructure formed, (see Fig. 9b). XRD results (Fig. 10a) show that the crystalline phase is lithium disilicate with no lithium metasilicate detected. By contrast, bulk gel-derived powders prepared with this solution crystallized into a mixture of lithium metasilicate and lithium disilicate [17]. The crystalline grains are much smaller than those in methoxyethoxide-based coatings, but they are still as large laterally as they are thick. Isothermal heating experiments at different temperatures were also carried out with the coatings prepared from the ethoxide route. However, AFM was less useful for following the crystallization process, because distinct partially crystallized microstructures were not observed. Instead, increasing the isothermal heating time led to some roughening of the surface and then the appearance of a fully crystallized microstructure. The average grain size in fully crystalline coatings was ca. 0.3 μm and did not vary much with film thickness and processing temperature. The smaller grain size and the faster crystallization observed in coatings prepared using ethoxide solution indicates that the nucleation rate is higher than that of coatings prepared using the methoxyethoxide solution. As discussed later, the difference may be due to the chemical homogeneity of the two solutions.

The microstructure of ethoxide-based coatings was modified by altering the synthesis procedure for the ethoxide stock solution. As previously reported, chemical heterogeneities which arise in ethoxide sols on the addition of the water-containing hydrolysis solution can be eliminated by using partially-hydrolysed TEOS in the solution preparation [17]. Gel-derived powders prepared by this route formed only the lithium disilicate on heating. Coatings prepared using the ethoxide route with partially-hydrolysed TEOS have a much different microstructure than that of the original ethoxide route. Fig. 11 shows an AFM micrograph of a coating after heating at 550 $^{\circ}\text{C}$ for 30 min. The coating is only partially crystallized and larger grains have formed in a manner similar to coatings prepared using the methoxyethoxide route. For this modified ethoxide-based route, complete crystallization requires higher temperatures and/or longer times. Lithium disilicate is the only crystalline phase found by XRD (Fig. 10b). No orientation effects were noted in either of the ethoxide-based coatings. The addition of nitric acid increased homogeneity in gel-derived powders [17] and dramatically increased the amount of lithium disilicate. Coatings prepared from ethoxide solution with addition of a small amount of HNO_3 ($[\text{HNO}_3/\text{Si} = 0.1]$) were also investigated. After heating at 550 $^{\circ}\text{C}$ for 30 min, the coating had a cloudy appearance and contained pin-holes and cracks. These defects may have been caused by the decomposition of the residual nitrate.

3.3. Effect of a seed layer

The microstructural differences between coatings prepared from Li-Si ethoxide and methoxyethoxide

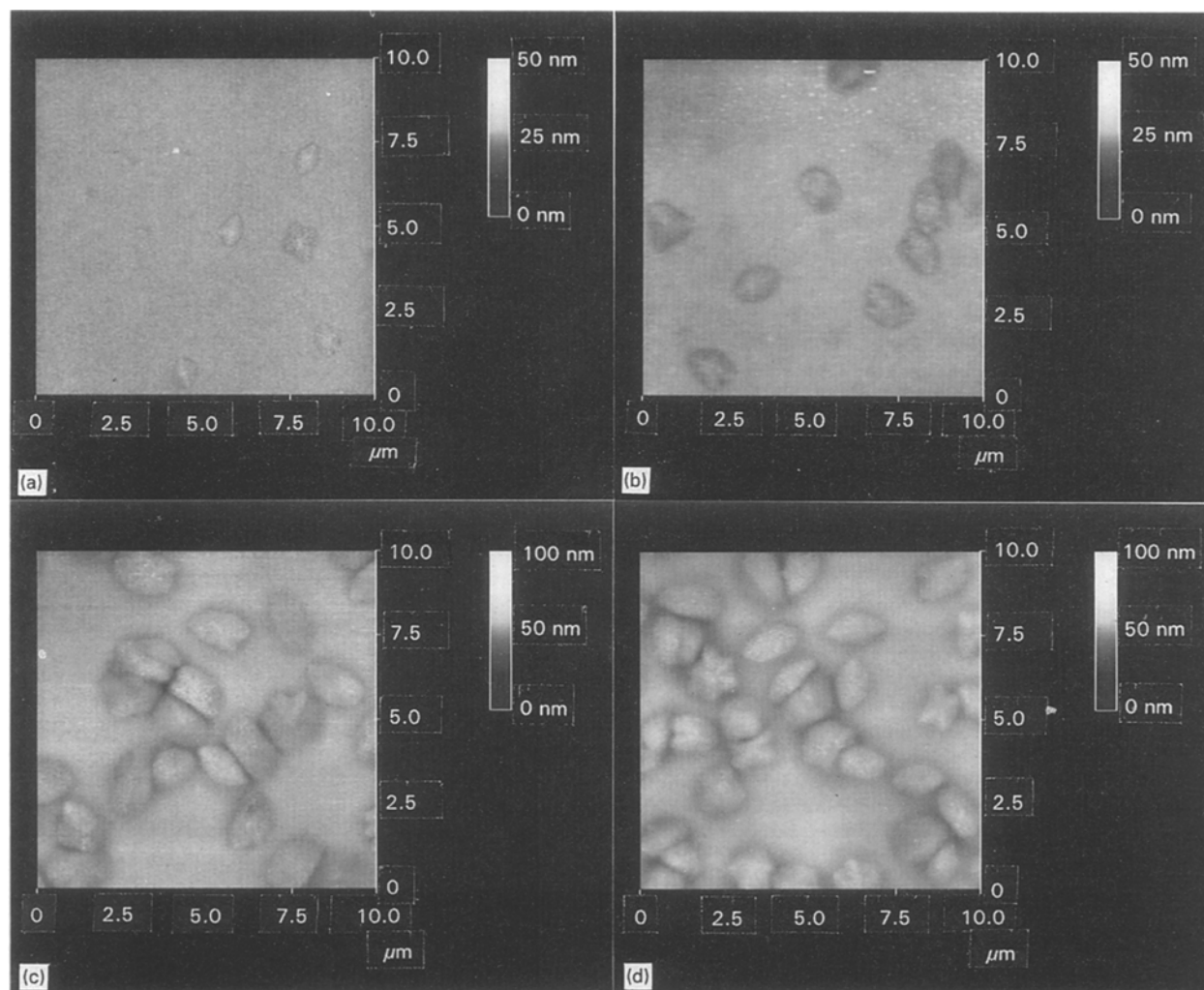


Figure 6 AFM micrographs of coatings prepared from the methoxyethoxide solution with different thicknesses (μm): (a) 0.04; (b) 0.08; (c) 0.17; and (d) 0.28. Coatings were prepared on Si and heated at 550°C for 30 min.

solutions offer an opportunity to tailor the final coating microstructure through the use of a “seed layer”. A single layer coating from the ethoxide route (without partially-hydrolysed TEOS) was prepared with two microstructures: (1) an amorphous, featureless microstructure (200°C , 1 min); and (2) a fine-grained, fully crystallized microstructure (550°C , 30 min). A methoxyethoxide-based coating was then deposited on to each ethoxide-based seed layer and heated at 550°C for 30 min. The thickness of the methoxyethoxide coating was roughly four times greater than that of the seed layer. When deposited and heated on both the amorphous and crystalline seed layers, this methoxyethoxide-based coating formed a fine-grained microstructure (see Fig. 12). Without the seed layer, similarly treated methoxyethoxide-based coatings had a larger grain size and a partially crystallized microstructure (Fig. 3a). The amorphous ethoxide-based seed layer effectively increased nucleation rate to give a finer grain size. The crystalline ethoxide-based seed layer also controlled the microstructure as it provided a source of heterogeneous nuclei.

The use of seed layers prepared from the Li–Si methoxyethoxide solution was also investigated. These seed layers were prepared on Si to give different microstructures: (1) amorphous, featureless (200°C ,

1 min); (2) large-grained, partially crystallized (550°C , 30 min); and (3) large-grained, fully crystallized (600°C , 30 min). Li–Si ethoxide solution (without partially-hydrolysed TEOS) was then deposited on to each of the seed layers and heated at 550°C for 30 min. Again, the top ethoxide-based coating was roughly four times thicker than the seed layer. A fine-grained microstructure developed in the ethoxide coating prepared on an amorphous seed layer (Fig. 13a); however, when a fully crystallized seed layer was used, the ethoxide coating developed into large-grained microstructure (Fig. 13c) which mimics the large-grained structure of the seed layer beneath. A microstructure with a bimodal grain size (Fig. 13b) was obtained when a partially crystallized seed layer was used. The portion of the coating with the crystalline material in the seed layer beneath apparently formed into larger crystalline grains while the portion with amorphous material beneath became a fine crystalline structure.

3.4. Effect of the substrate

Fig. 14 shows the microstructures of coatings prepared by depositing Li–Si methoxyethoxide solution on to a variety of substrate materials and heating at 550°C for 30 min. In addition to Si (discussed above),

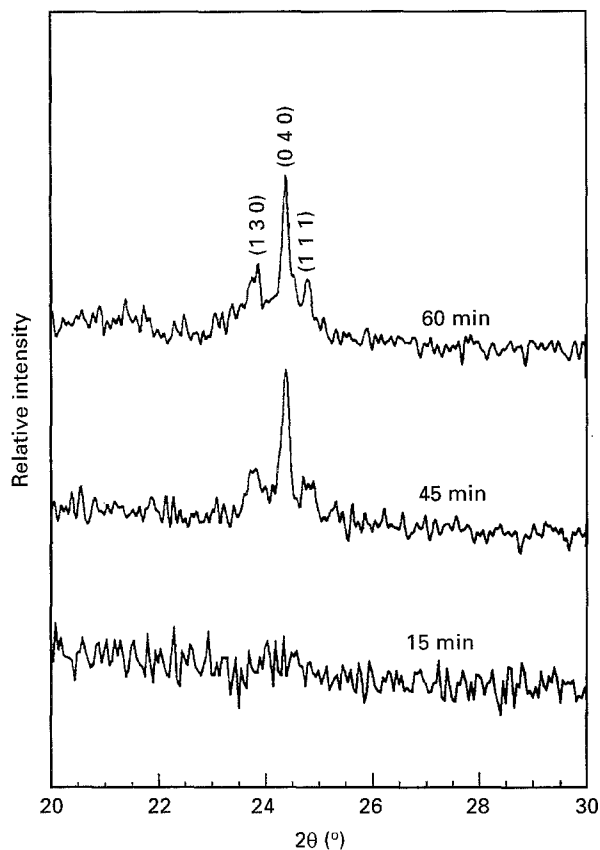


Figure 7 X-ray diffraction results for coatings prepared using the methoxyethoxide solution and heated at 550°C for the times given. Indexed peaks are for lithium disilicate.

Si with a thermal oxide (ca. 100 nm), Si with a layer of polycrystalline Si (ca. 550 nm) and (000 1) sapphire were investigated. Coatings prepared on polycrystalline Si (Fig. 14a) and sapphire (Fig. 14b) had microstructures with fine grain sizes and were fully crystallized. Coatings prepared by the ethoxide route on crystalline substrates (e.g. Si and sapphire) had similar fully crystallized microstructures with fine grain sizes. The microstructure of methoxyethoxide-based coatings on Si with native oxide and Si with the

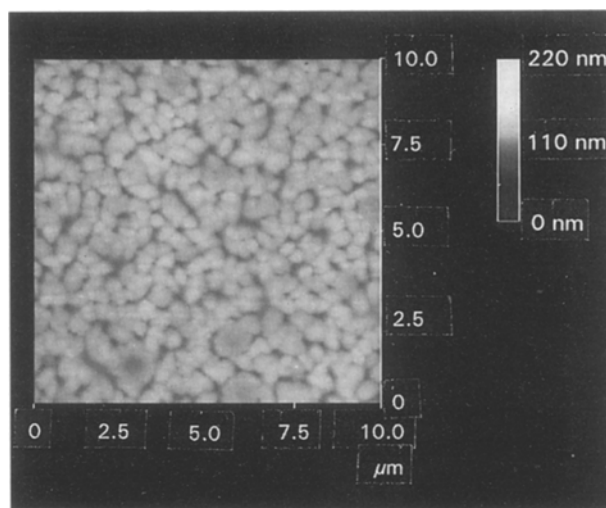


Figure 8 AFM micrograph showing the microstructure of a coating prepared on Si from methoxyethoxide solution with addition of a small amount of H_2PtCl_6 and heated at 550°C for 30 min. Coating thickness is ca. 0.2 μm .

thicker thermal oxide were virtually identical (i.e. partial crystallinity and larger grains after 30 min at 550°C). These results indicate that the crystalline substrates were effective at increasing the number of nucleation sites.

Coatings prepared on sapphire substrates had extremely fine grained microstructures. An AFM micrograph of an annealed sapphire substrate (Fig. 14d) shows facets that develop during the annealing treatment. As-received sapphire substrates not shown were featureless. The microstructures of Li-Si methoxyethoxide coatings heated at 550°C for 30 min on these two types of sapphire substrates were different. On annealed substrates, the fine grains appear to form in parallel rows with a spacing about the same as the facet spacing (see Fig. 14c). XRD results for coatings (Fig. 15) prepared on as-received and annealed sapphire substrates show differences in orientation. The most intense peaks for the lithium disilicate coatings were (1 3 0) and (2 0 0), and also for coatings

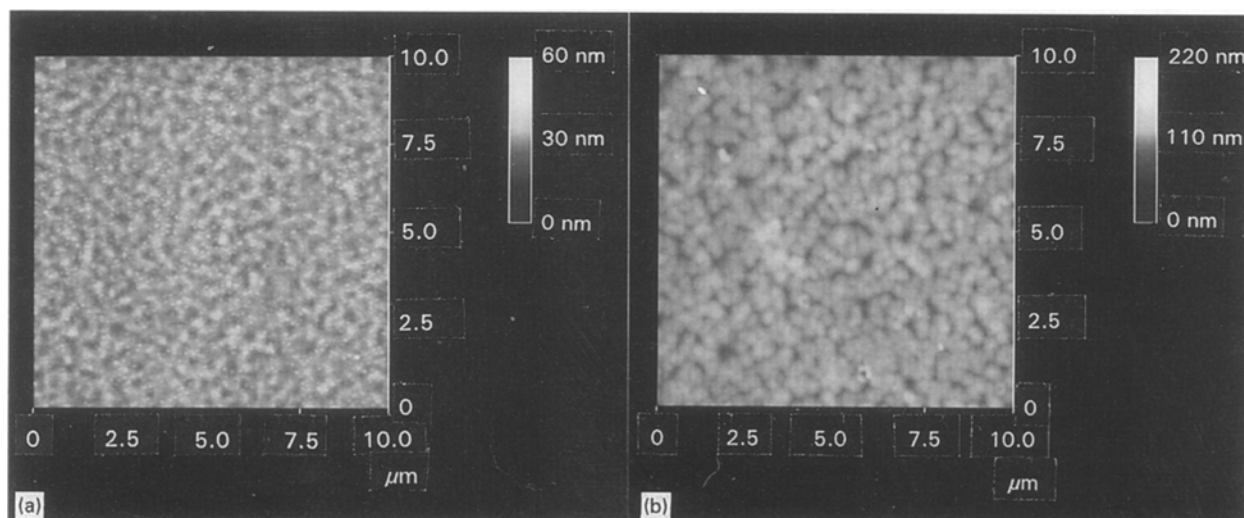


Figure 9 AFM micrographs of coating prepared using the ethoxide solution and heating at: (a) 500°C for 1 h; and (b) 550°C for 15 min. Coating thickness is 0.1 μm .

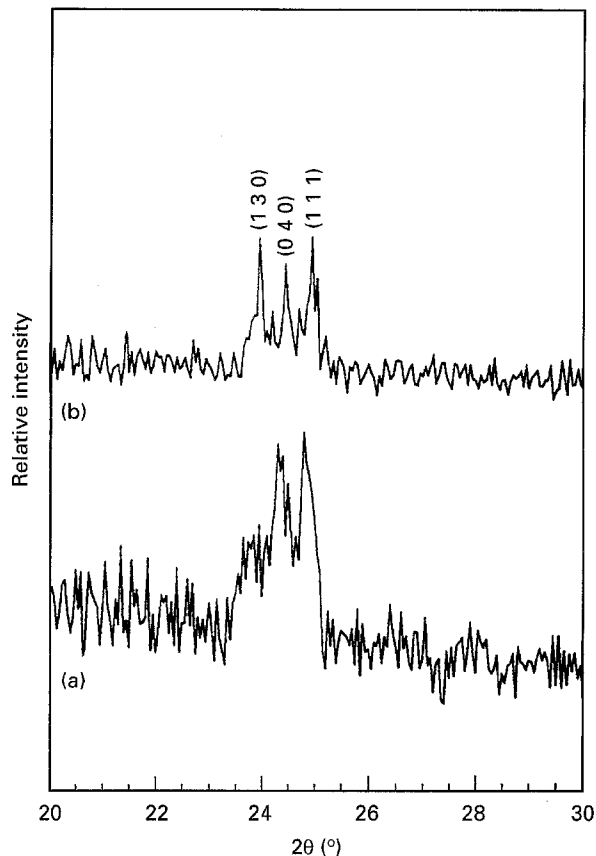


Figure 10 XRD of coatings prepared using: (a) the ethoxide solution and (b) the ethoxide solution with partially-hydrolysed TEOS. Coatings (0.1 μm thick) were prepared on Si and heated at 550 $^{\circ}\text{C}$ for 30 min. Indexed peaks are for lithium disilicate.

prepared on the annealed sapphire substrate, peaks (110) and (040) were missing.

4. Discussion

The crystallization behaviour and the microstructure development in sol-gel-derived lithium disilicate coatings are strongly affected by the coating solution

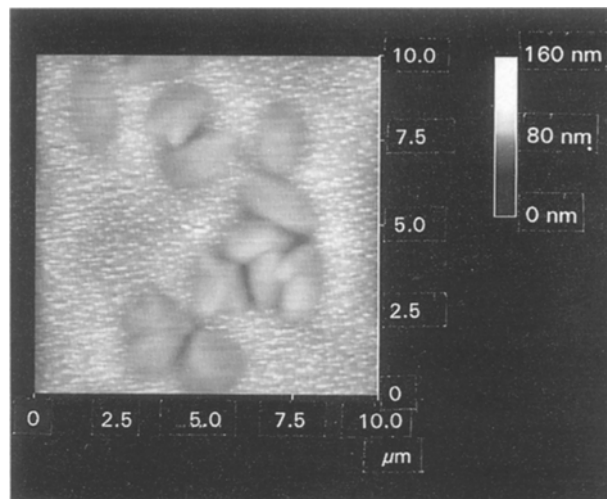


Figure 11 AFM micrograph showing the microstructure of a coating prepared using ethoxide solution with partially-hydrolysed TEOS and heated at 550 $^{\circ}\text{C}$ for 30 min. Coating thickness is 0.1 μm .

chemistry, thermal treatment conditions, coating thickness and substrate material. The final microstructure may also be controlled using a seed layer with “designed” chemistry and crystallinity.

Isothermal crystallization experiments on the methoxyethoxide-based coatings prepared on Si substrates revealed trends in microstructure which are related nucleation and crystal growth behaviour. At 550 $^{\circ}\text{C}$, the amorphous-to-crystalline transformation takes place gradually with grains growing in the amorphous coating. The grains grow to a large lateral dimension (2–5 μm), although the coating is thin (ca. 0.2 μm). The growth occurs during the transformation; heating beyond full crystallization and spherulite impingement does not increase the grain size significantly. From cross-sectional TEM, the grains clearly span the thickness of the coating. Considering that each grain originates from a nucleus, the number of nuclei is very small to achieve grains of such large

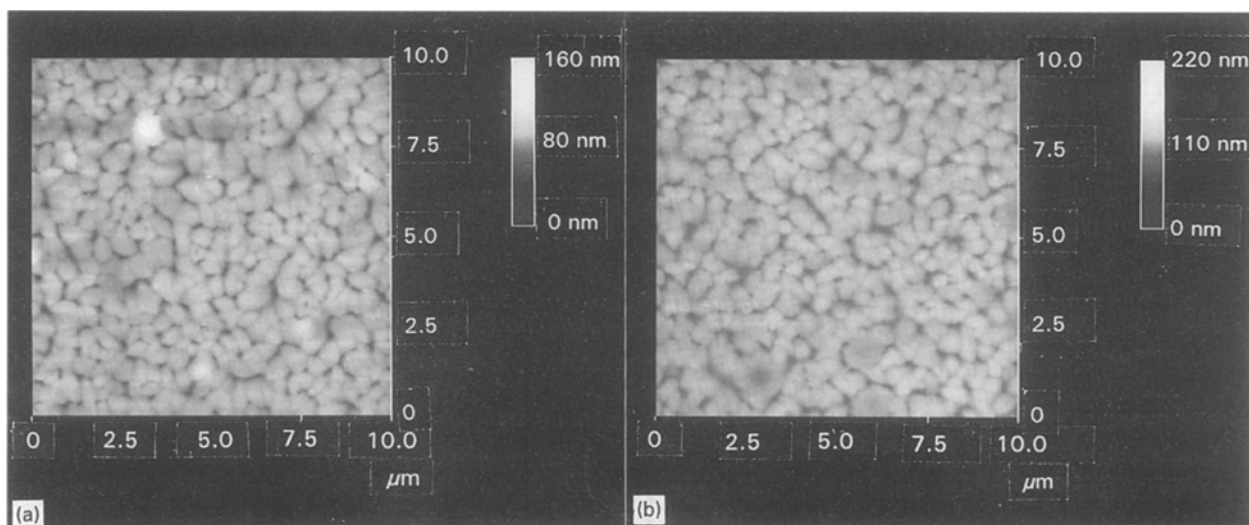


Figure 12 AFM micrographs showing the microstructures of methoxyethoxide-based coatings deposited on ethoxide-based seed layers and heated at 550 $^{\circ}\text{C}$ for 30 min: (a) an amorphous seed layer and (b) a fully crystallized, fine-grained seed layer.

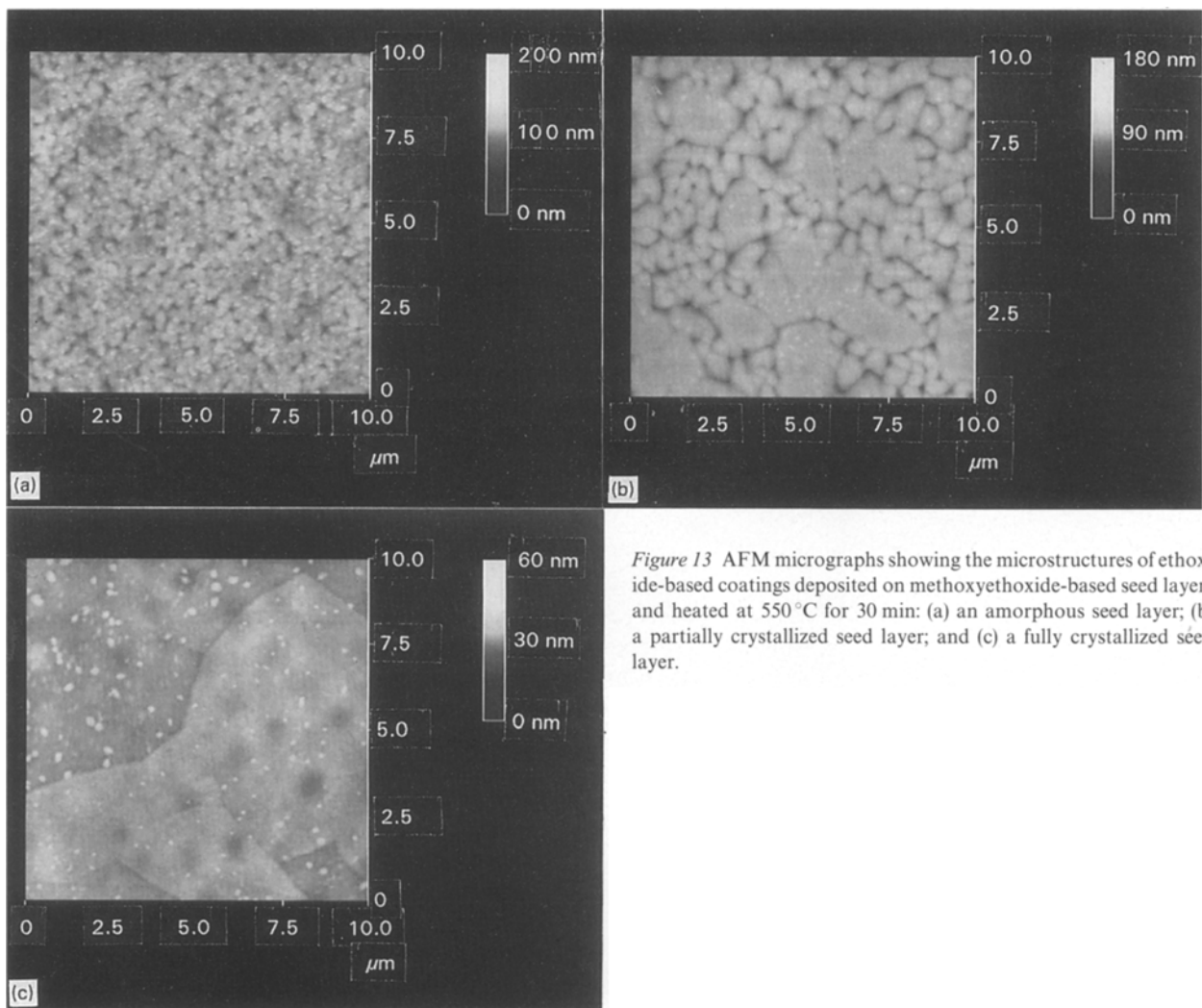


Figure 13 AFM micrographs showing the microstructures of ethoxide-based coatings deposited on methoxyethoxide-based seed layers and heated at 550 °C for 30 min: (a) an amorphous seed layer; (b) a partially crystallized seed layer; and (c) a fully crystallized seed layer.

dimensions and the nuclei must be widely separated. The transformation rate increased dramatically at temperatures slightly higher than 550 °C (i.e. 575 and 600 °C). Despite the difference in the transformation rate, there was little difference in grain size for fully crystalline coatings prepared at different temperatures. Therefore, the number of nuclei appears to be independent of the isothermal heating temperature. A thickness dependence was also noted; thicker coatings displayed a faster transformation rate, a greater number of grains per unit area and a finer average grain size after full crystallization. From these observations, it can be concluded that the number of nuclei increase with coating thickness, allowing speculation on the nucleation mechanism.

Several nucleation mechanisms are possible in sol-gel coatings, including nucleation at the surface, in the coating (homogeneous and heterogeneous), and heterogeneous nucleation at the coating-substrate interface. For the methoxyethoxide coatings on Si, nucleation exclusively at the coating-substrate interface or at the surface is not likely because these mechanisms would probably provide an equal number of nuclei regardless of the thickness. Homogeneous or heterogeneous nucleation in the coating could cause an increase in the number of nuclei with coating thickness. Homogeneous nucleation, while uncom-

mon in coatings, generates greater numbers of nuclei in thicker coatings due to their greater volume. Heterogeneous sites in the coating could arise from the incorporation of defects, such as dust, during the multilayer coating process used to prepare thick coatings. Experimental results show that thicker coatings have a higher fraction of the crystalline phase for a given heat treatment. In a theoretical treatment of homogeneous nucleation in thin films of finite volume, Weinberg [27] demonstrated that the greater number of nuclei in thicker films (larger volumes) causes the faster transformation; presumably the same would be true for heterogeneous sites in the coating. After complete crystallization, the final grain size is larger in thinner coatings than in thicker coatings. Thinner coatings have fewer nuclei that are necessarily separated by greater distances so that grains grow laterally to greater dimensions before impingement.

AFM and TEM observations of the microstructures of both methoxyethoxide- and ethoxide-based coatings revealed that the crystalline grains grow as spherulites. Such a growth pattern is common for bulk lithium disilicate prepared from the melt-derived glasses [22, 23] and agrees with the general observation that spherulitic growth is favoured in multi-component systems with low nucleation rates [22]. The low nucleation rate in the coatings prepared using

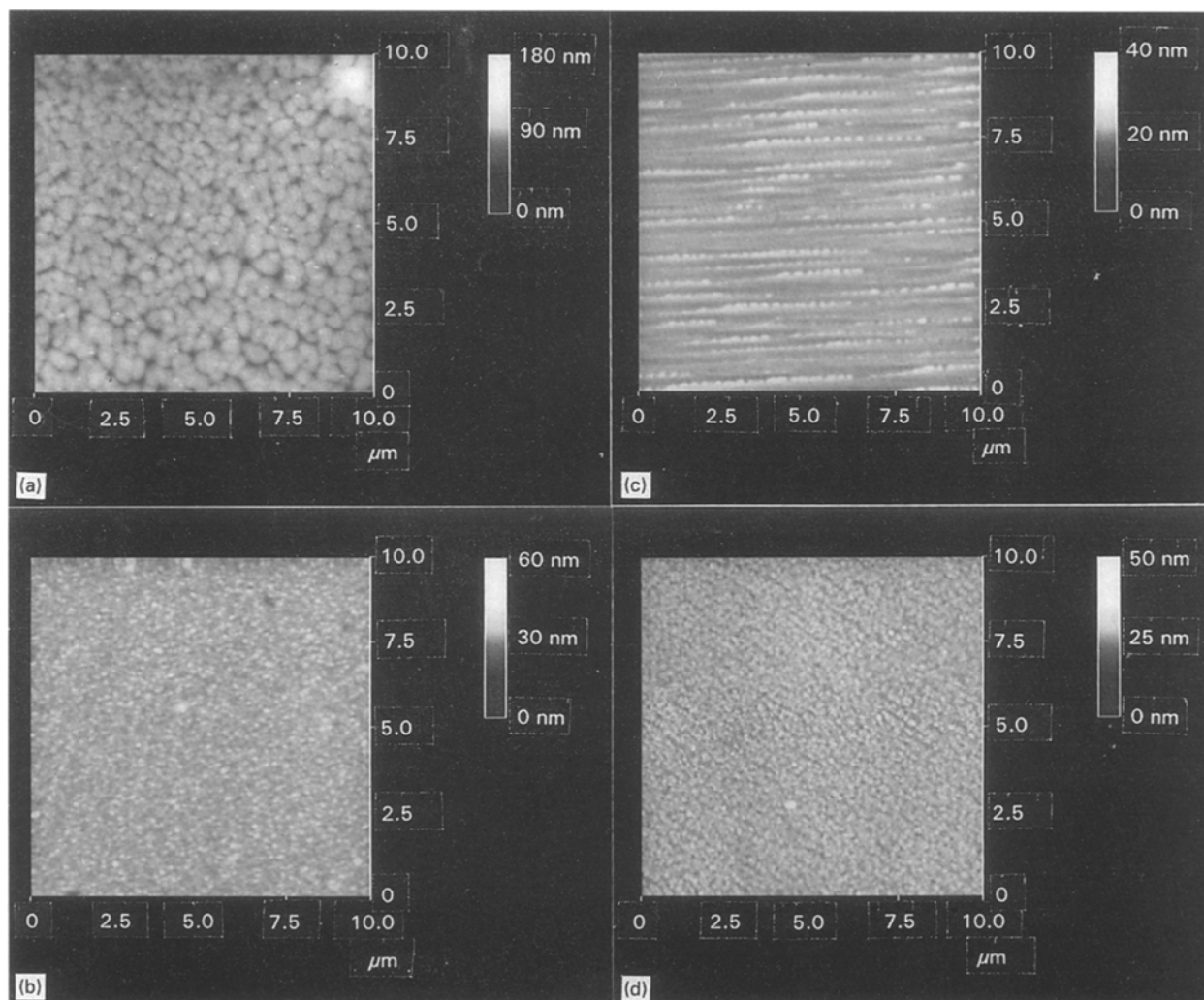


Figure 14 AFM micrographs showing the surface morphology of fully crystallized microstructures of the methoxyethoxide-based coatings on: (a) poly Si; (b) as-received sapphire; and (c) the surface morphology of annealed sapphire substrate. (d) Annealed sapphire (1400 °C for 2 h in air) substrates. All coatings are 0.2 μm thick and were heated at 550 °C for 30 min.

Li–Si methoxyethoxide solution leads to the formation of grains that span the thickness of the coating and grow to large lateral dimensions. The ellipsoidal grains take on a preferred orientation with the lithium disilicate *b*-axis perpendicular to the plane of the coating. $\text{Li}_2\text{Si}_2\text{O}_5$ is orthorhombic with a layered structure composed of Si_2O_5 sheets in the *a*–*c* plane with Li cations between sheets. Rowland and James [28] postulated that the differences in bonding within and between sheets leads to differences in surface energy and hence preferential formation of plate-like, oriented grains. Preferred orientation in coatings may also be a consequence of these surface energy effects. The shape of crystalline grains changes from ellipsoidal to irregular in the later stage of growth as the spherulitic grains impinge. After impingement the growth rate is low because the driving force for growth is reduced. Thompson [29] reports that normal grain growth is not energetically favourable in fully crystalline coatings with a columnar structure once the grain size is greater than the coating thickness. In ethoxide-based coatings, the high nucleation rate (see below) gives rise to a larger number of nuclei and smaller grains. Again, impingement of these fine grains inhibits the rate of grain growth.

A comparison of crystallization behaviour in coatings prepared on Si shows the effects of solution chemistry. Coatings prepared using Li–Si methoxyethoxide solution began to show crystallinity after heating at 500 °C for 8 h. By contrast, similar coatings prepared using Li–Si ethoxide solution started to crystallize much sooner, after only 1 h at 500 °C. For ethoxide-based coatings, full crystallization into a fine-grained microstructure was achieved after heating at 550 °C for 30 min. The same thermal treatment on methoxyethoxide coatings (0.2 μm thick) resulted in a large-grained, partially crystallized microstructure. These observations indicate that the nucleation rate is higher in the ethoxide-based coatings as compared with methoxyethoxide-based coatings. The higher nucleation rate is most likely related to chemical heterogeneity in the ethoxide coating solution. When the Li–Si ethoxide solution is combined with the water-containing hydrolysis solution, a fast reaction between Li ethoxide and water results in the formation of a fine white LiOH precipitate [17]. The precipitate eventually dissolves to give a clear solution; however, precipitation can lead to local chemical heterogeneity. If silicate species condense while lithium is isolated in the precipitate phase, local Si-rich and Li-rich

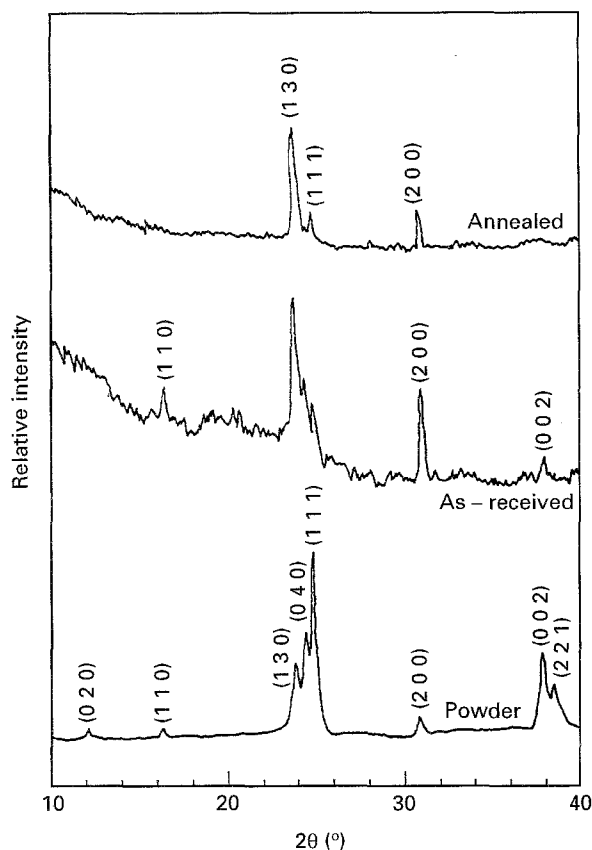


Figure 15 XRD results for methoxyethoxide-based coating prepared on (a) an annealed sapphire substrate and (b) an unannealed sapphire substrate. The coating was heated at 550 °C for 30 min.

regions form. The heterogeneity was very apparent in gel-derived powders (prepared with $r = 3-5$) which crystallized into lithium metasilicate (Li_2SiO_3) in addition to lithium disilicate on heating [17]. For coatings, only the lithium disilicate phase was detected by XRD. The lesser amount of water in the coating solution ($r = 2$), and perhaps the more rapid solidification of the coating, made the problem less severe, but even a small amount of lithium metasilicate (i.e. an amount less than the detection limit of the XRD) could increase the nucleation rate [30].

Changes in the chemistry of both the Li-Si ethoxide and Li-Si methoxyethoxide solutions strongly affected the nucleation rate and microstructure. Ethoxide-based solutions prepared using partially-hydrolysed TEOS did not suffer the LiOH precipitation because the partially hydrolysed silicate species reacted with the Li ethoxide before water was added [17]. Coatings prepared from these solutions formed into large-grained microstructures upon heating. Similar to those prepared using the methoxyethoxide-based solution, slower crystallization with distinct partially crystallized microstructures was observed. The use of partially-hydrolysed TEOS prevented LiOH precipitation and increased the homogeneity of the coating so that the nucleation rate was reduced. On the other hand, coatings made from the methoxyethoxide-based solution could be fashioned into a fine-grained microstructure through the intentional addition of a nucleation agent, H_2PtCl_6 (which decomposes to form Pt during heating). The rate of transformation was higher

in the coatings with the additive and the final microstructure contained fine grains, rather than the usual large grains. Lithium disilicate nuclei form favourably around the Pt particles to reduce interfacial energy. Similar behaviour can be found in lithium silicate bulk glasses. Rindone [31] reported that adding a small number of Pt particles to lithium silicate glass increased the crystallization rate of lithium disilicate. Moreover, the crystallization rate went through a maximum when an optimum amount of Pt was used and crystallization of lithium disilicate was favoured by Pt particles of small size.

The final microstructure of coatings was also affected by the substrate material. Methoxyethoxide-based coatings prepared on Si with native or thermal oxide had similar microstructures with large grains; identical coatings on poly Si and sapphire substrates yielded very fine-grained microstructures which were fully crystallized at lower temperatures or shorter times. Crystalline substrates provide a multitude of heterogeneous nucleation sites. The physical nature of the substrate surface (i.e. impurities, steps, scratches, grain boundaries and inclusions) affect the crystallization rate of the coatings. The substrate surface defects are known to act as preferential nucleation sites, resulting in an increased nucleation rate [32]. The annealed (0001) sapphire substrates were especially interesting as the lithium disilicate grains aligned in the same way as the facets on the substrate. XRD results for coatings on both as-received and annealed sapphire substrates showed strong (130) and (200) orientations. Sapphire has a hexagonal crystal structure; the unit cell parameter of the basal plane is 0.476 nm. The c lattice parameter of the orthorhombic lithium disilicate crystal structure (0.487 nm) matches the basal plane of the sapphire substrate. Hence, some planes containing the c -axis (i.e. $(hk0)$ planes) have a more favourable orientation. For coatings on annealed substrates, the peaks for (130) and (200) are still strong, but the peaks for (110) and (040) are diminished. Susintzky and Carter [33] reported that the formation of facets of plane $(11\bar{2}0)$ is favoured on annealed sapphire substrate to reduce the surface energy. There appears to be no crystallographic relationship between this plane and the strong or absent peaks; therefore, the preferred orientation on the annealed substrate may also be related to surface energy effects.

The seed layer experiments are further evidence for the different mechanisms for the ethoxide- and methoxyethoxide-based coatings, and provide interesting examples of microstructure tailoring. The amorphous ethoxide-based seed layer caused a methoxyethoxide-based coating on top to form a fine-grained microstructure. In this case, the seed layer nucleated first and provided nucleation sites for the coating. By contrast, an amorphous methoxyethoxide-based seed layer did not influence the microstructure of the ethoxide-based coating; here, nucleation took place in the ethoxide-based coating and was not effected by the seed layer. A crystalline, large-grained seed layer prepared from the methoxyethoxide precursor served as a more effective nucleation source, causing the ethoxide-based coating to form into

a large-grained microstructure. The crystalline seed layer provided a template for nucleation and growth of the coating. These experiments show that microstructural features can be tailored into coatings using very thin seed layers. Since some properties are influenced by grain size, opportunities exist for using the seed layer approach to achieve desirable microstructures.

5. Summary

The microstructure of sol-gel-derived lithium disilicate coatings prepared on Si substrates depended on the chemistry of the alkoxide solution and coating thickness, in some cases. Coatings prepared from Li-Si methoxyethoxide tended to crystallize into large grains (2–5 μm), although the coating was very thin (<0.3 μm). At temperatures at or below 550 °C, the transformation was gradual so that partially crystalline microstructures were observed. The growth of the grains was halted by spherulite impingement at full crystallization. Thicker coatings had a larger number of grains per unit area, transformed faster and had finer grain sizes after complete crystallization. The formation of large grains indicates a low nucleation rate and the thickness dependence requires that the nuclei form through the thickness of the coating by homogeneous or heterogeneous mechanisms. Introducing a nucleation agent (Pt) increased the nucleation rate and led to a fine-grained microstructure. As compared with the methoxyethoxide-based coatings, coatings prepared from Li-Si ethoxide solution crystallized into microstructures with fine grains (<0.5 μm). In this system, chemical heterogeneity linked to the formation of lithium hydroxide precipitate is suspected as the cause for an increased nucleation rate. Microstructures similar to the methoxyethoxide coatings were achieved when the solution processing was changed to eliminate the precipitate.

The substrate and the presence of a seed layer influenced microstructure development. On crystalline substrates (poly Si, sapphire), all coatings developed into very fine-grained structures, with sapphire generating the smallest grain size. The crystalline surface provided sites for heterogeneous nucleation. On amorphous surfaces, such as Si with native or thermal oxide, the chemistry of the coating appeared to have a greater influence on the microstructure. The chemistry effects allowed the use of a "seed layer" to tailor the coating microstructure. Amorphous seed layers, with higher nucleation rates than the coatings on top, control the microstructure of the coating, while seed layers with lower nucleation rates are ineffective. Crystalline seed layers served as templates for the nucleation and growth of the coating on top.

Acknowledgement

Support from the NSF of Center for Interfacial Engineering is gratefully acknowledged.

References

1. M. H. FREY and D. A. PAYNE, *Appl. Phys. Letters* **63** (1993) 2753.
2. L. F. FRANCIS and D. A. PAYNE, *J. Amer. Ceram. Soc.* **74** (1991) 3000.
3. A. R. DI GIAMPALOLO CONDE, M. PUERTA, H. RUIZ and J. LIRA OLIVARES, *J. Non-Cryst. Solids* **147 & 148** (1992) 467.
4. L. F. FRANCIS, in "Intermetallic and Ceramic Coatings", edited by T. S. Sudarshan and N. D. Dahotre (Marcel Dekker, New York, in press).
5. C. J. BRINKER and G. W. SCHERER, "Sol-gel science: the physics and chemistry of sol-gel processing" (Academic Press, New York, 1990).
6. R. A. CAIRCROSS, L. F. FRANCIS and L. E. SCRIVEN, *Drying Technol. J.* **10** (1992) 893.
7. V. JOSHI and M. L. MECARTNEY, *J. Mater. Res.* **8** (1992) 2668.
8. J. L. KEDDIE, P. V. BRAUN and E. P. GIANNELIS, *J. Amer. Ceram. Soc.* **77** (1994) 1592.
9. R. W. SCHWARTZ, J. A. VOIGT, C. D. BUCHHEIT and T. J. BOYLE, in "Ferroic materials: design, preparation and characteristics", edited by A. S. Bhalla, K. M. Nair, I. K. Lloyd, H. Yanagida and D. A. Payne (American Ceramic Society, Westerville, OH, 1994) p. 145.
10. K. MATUSITA and M. TASHIRO, *J. Non-Cryst. Solids* **11** (1973) 471.
11. M. C. WEINBERG and E. D. ZANOTTO, *ibid.* **108** (1989) 99.
12. A. R. HYDE, G. PARTRIDGE and S. VIGNESOULT, *Brit. Ceram. Trans.* **92** (1993) 55.
13. R. DUPREE, D. HOLLAND and M. G. MORTUZA, *J. Non-Cryst. Solids* **116** (1990) 148.
14. G. J. GARDOPEE, R. E. NEMNHAM and A. S. BHALLA, *Ferroelectrics* **33** (1981) 155.
15. J.-M. WU, W. R. CANNON and C. PANZERA, US Patent 4515 634.
16. S. P. SZU, L. C. KLEIN and M. GREENBLATT, *J. Non-Cryst. Solids* **121** (1990) 90.
17. P. LI, B. FERGUSON and L. F. FRANCIS, *J. Mater. Sci.* submitted.
18. E. PRESTON and W. E. S. TURNER, *J. Soc. Glass Technol.* **18** (1934) 143.
19. D. E. VEINOT, K. B. LANGILLE, D. T. NGUYEN and J. O. BERNT, *J. Non-Cryst. Solids* **127** (1991) 221.
20. T. WANG, C. LEE and L. D. SCHMIDT, *Surf. Sci.* **163** (1985) 181.
21. I. M. REANEY and D. J. BARBER, *J. Amer. Ceram. Soc.* **74** (1991) 1635.
22. P. F. JAMES, *Phys. Chem. Glasses* **15** (1974) 95.
23. V. KOMPPA, *ibid.* **20** (1979) 130.
24. M. H. LEWIS and G. SMITH, *J. Mater. Sci.* **11** (1976) 2015.
25. H. D. KEITH and F. J. PADDEN, *J. Appl. Phys.* **44** (1963) 2409.
26. E. M. LOGOTHETIS and W. J. KAISER, *Sensors and Actuator* **4** (1983) 333.
27. M. C. WEINBERG, *J. Non-Cryst. Solids* **72** (1985) 301.
28. E. G. ROWLAND and P. F. JAMES, *Phys. Chem. Glasses* **20** (1979) 9.
29. C. V. THOMPSON, *Ann. Rev. Mater. Sci.* **20** (1990) 245.
30. L. L. HENCH, S. W. FRIEMAN and D. L. KINSER, *Phys. Chem. Glasses* **21** (1971) 58.
31. G. E. RINDONE, *J. Amer. Ceram. Soc.* **45** (1962) 7.
32. T. SPALVINS and W. A. BRAINARD, *NASA Technical Memorandum* **28** (1974) 521.
33. D. W. SUSNITZKY and C. B. CARTER, *J. Amer. Ceram. Soc.* **75** (1992) 2463.

Received 2 February
and accepted 24 May 1995